The Parameters of the Gamma-Ray Emission Region in Mrk 501

W. Bednarek[1,2] and R.J. Protheroe[1]
[1] *University of Adelaide, Dept. of Physics & Math.Physics, Adelaide, SA 5005, Australia*
[2] *University of Łódź, 90-236 Łódź, ul. Pomorska 149/153, Poland*

Abstract

We determine the physical parameters (magnetic field and Doppler factor) of the homogeneous synchrotron self-Compton model allowed by the observed X–ray to gamma-ray spectra and variability of Markarian 501 during the 15–16 April 1997 flaring activity. We find that, for 20 minute variability, a magnetic field of 0.2 G and a Doppler factor of 20 could fit these observations. We take account of photon-photon pair production interactions of gamma-ray photons occurring both inside the emission region and during propagation to Earth and find these to be extremely important in correctly determining the allowed model parameters.

1 Introduction:

The spectrum of Mrk 501 shows clear curvature over 0.3–10 TeV (Krennrich 1998), and extends up to 24 TeV (Konopelko et al. 1999, Krawczynski et al. 1999). The γ-ray emission of Mrk 501 showed evidence of variability on a time scale of 20 minutes (Aharonian et al. 1998). The TeV γ-ray flares are simultaneous with the X-ray flares, and during the 16 April 1997 flare the X-ray spectrum was observed by the Beppo-SAX observatory up to $\sim$ 200 keV (Pian et al. 1998), and during the same high state OSSE observations (Catanese et al. 1997) showed that the energy flux per log energy interval continued up to $\sim$ 500 keV at roughly the same level.

Gamma-ray emission from active galactic nuclei (AGN) is often interpreted in terms of the homogeneous "synchrotron self-Compton model" (SSC) in which the low energy emission (from radio to X-rays) is synchrotron radiation produced by electrons which also up-scatter these low energy photons into high energy γ-rays by inverse Compton scattering (ICS).

The inclusion of photon-photon pair production interactions of γ-rays with low energy radiation within the emission region has been used previously when constraining the physical parameters of blazars (e.g. Mattox et al. 1993, Dondi & Ghisellini 1995, Bednarek and Protheroe 1997). However in recent work on Mrk 501 by various authors (Kataoka et al. 1999, Tavecchio, Maraschi and Ghisellini 1998) absorption on both the infrared background (IRB) and the internal radiation of the emission region has been neglected. We show that inclusion of both these effects is vital. Full details and additional references to observations and earlier work are given by Bednarek and Protheroe (1999).

2 Absorption of Gamma-Rays by Photon Photon Pair Production

We use the upper and lower IRB models of Malkan and Stecker (1998) to obtain the optical depth, $\tau_{\rm IR}(E_\gamma)$, in the IRB plus cosmic microwave background radiation. Fig. 1 shows the 1997 April 15–16 HEGRA and CAT data together with the approximation used later in this paper for the high energy part of the spectral energy distribution (SED). The figure also shows this SED after correction for absorption in the infrared using the two IRB models.

Absorption of γ-rays will also take place on the synchrotron photons produced inside the emission region. For the spectrum of these target photons we use a fit to the Beppo-SAX observations extended to $\varepsilon_{\rm s,max} = 500$ keV. We assume that relativistic electrons are confined inside a "blob" which moves along the jet with Doppler factor D and has magnetic field B. In the homogeneous SSC model the radii of the emission regions of low energy photons (r_l), X-ray photons (r_X), and TeV γ-rays (r_γ)

are the same. This region is constrained by the variability time scale observed, e.g. in TeV γ-rays, $t_{\rm var}$, by $r_l = r_\gamma = r_X \approx 0.5cDt_{\rm var}$. The differential photon density in the blob frame of synchrotron photons is then given by $n(\varepsilon') \approx [4d^2F(\varepsilon)]/(c^3t_{\rm var}^2D^4)$, where $\varepsilon = D\varepsilon'$ and ε' are the photon energies in the observer's and the blob rest frames. From numerical integration, we obtain the optical depth for $e^\pm$ production $\tau_{\rm syn}(E'_\gamma)$ in the blob frame, for γ-ray photons with blob-frame energy $E'_\gamma = E_\gamma/D$, as a function of D, and find its inclusion to be extremely important.

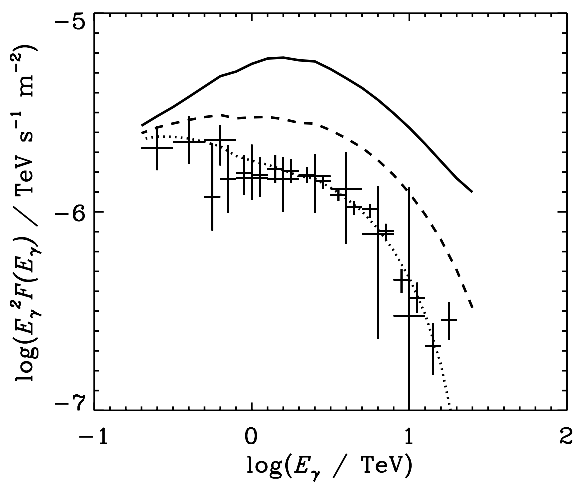

Figure 1: *Mrk 501 1997 April 15–16 HEGRA data (data binned in 1/10 decade intervals) and CAT data (Djannati-Atai A. et al., 1998; data binned in 1/5 decade intervals). The error bars on the HEGRA data include systematic errors as given in fig. 1b of Krawczynski et al. (1999). The dotted curve shows the SED used in this paper, and the solid and dashed curves show the SED after correction for absorption using the upper and lower IRB models.*

3 Constraints from Ratio of Gamma-Ray to X–ray Power

The spectrum of Mrk 501 shows two clear bumps which, during the outburst stage, extend up to at least ~ 500 keV (Catanese et al. 1997), and up to ~ 24 TeV (Konopelko et al. 1999, Krawczynski et al. 1999). These multiwavelength observations of Mrk 501 allow us to define the ratio η of the energy flux per log energy interval observed at a chosen γ-ray energy, $E_\gamma = 1$ TeV, at which the emission is assumed to be due to Compton scattering, to that at a chosen X–ray energy, $\varepsilon = 2$ keV, at which the emission is assumed to be due to synchrotron radiation,

$$\eta = (\frac{dN}{dE_\gamma dt}E_\gamma^2 e^{-\tau_{\rm tot}(E_\gamma)})/(\frac{dN}{d\varepsilon dt}\varepsilon^2) = (\frac{dN}{dE'_\gamma dt'}E'^2_\gamma e^{-\tau_{\rm tot}(E'_\gamma)})/\frac{dN}{d\varepsilon' dt'}\varepsilon'^2), \quad (1)$$

where $\tau_{\rm tot}(E_\gamma) = \tau_{\rm syn}(E_\gamma) + \tau_{\rm IR}(E_\gamma)$ is the total optical depth, and the primed quantities are measured in the blob frame.

The characteristic energy of synchrotron photons in the blob frame is given by $\varepsilon' \approx 0.5\varepsilon_B\gamma'^2$, where $\varepsilon_B = m_ec^2B/(4.4\times10^{13}$ G), and we use this together with the observed low energy SED to estimate the blob-frame equilibrium electron spectrum for various assumed B and D. We then use this electron spectrum to obtain the blob-frame synchrotron energy flux at $\varepsilon' = 2/D$ keV, and the IC energy flux at $E'_\gamma = 1/D$ TeV, as a function of B and D. We substitute these, together with $\tau_{\rm tot}(E_\gamma)$, into Eq. 1, and setting $\eta = 3.6$ (as observed), we obtain numerically B as a function of D plotted in Fig. 2(a) for $t_{\rm var} = 20$ minutes.

4 Constraints from Time Scales and Maximum Energies

The observed rapid decrease in the TeV γ-ray and X-ray fluxes may only occur if the electrons have sufficient time to cool during the flare, $t'_{\rm cool} \le t_{\rm var}D$. We consider the cooling time of electrons responsible for synchrotron radiation observed at 2 keV, i.e. having $\gamma' = (2\varepsilon/D\varepsilon_B)^{1/2}$, with $\varepsilon = 2$ keV. The cooling time scales for synchrotron and IC losses of electrons with Lorentz factor γ' are given by

$$t'^{\rm syn}_{\rm cool} = \frac{m_ec^2}{kU_{\rm mag}\gamma'}, \quad t'^{\rm ICS}_{\rm cool} \approx \frac{m_ec^2}{kU_{\rm rad}(<\varepsilon'_T)\gamma'}, \quad k = 4c\sigma_T/3, \quad (2)$$

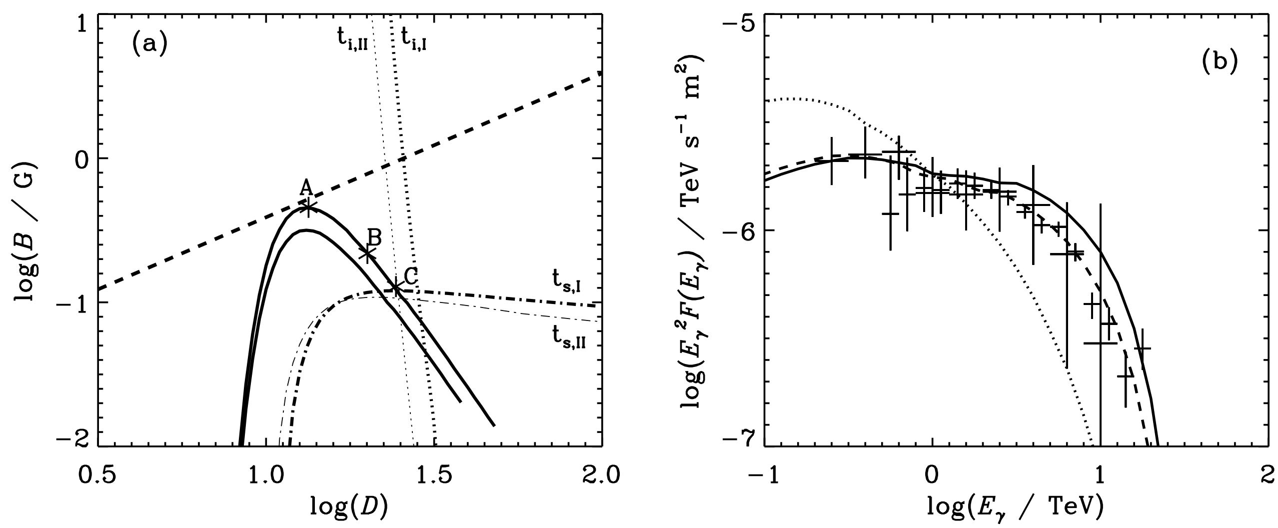

Figure 2: *(a) Constraints on the parameters of the blob assuming a variability time scale of* $t_{\rm var} = 20$ *min. The full curves give the allowed values for B and D constrained by Eq. 1 for the case of absorption of* γ*-ray photons in the IRB using the lower model (upper curve) and the upper model (lower curve), the dot-dashed curves give the lower limit from the synchrotron cooling time scale and the dotted lines give the upper limit from the inverse Compton cooling time scale for electrons with energies which produce synchrotron photons with observed energies of 2 keV (thick lines marked by* $t_{s,I}$ *and* $t_{i,I}$*) and 0.2 keV (thin lines marked by* $t_{s,II}$ *and* $t_{i,II}$*), and the dashed curve gives an upper limit from the maximum energies of synchrotron and inverse Compton photons. (b) Gamma-ray spectra computed for the specific values of B and D using the lower IRB model are compared with the observations of Mrk 501 in the 15-16 April 1997 flare. Dotted curves, dashed curves, and solid curves correspond to the points labelled A, B, and C in part (a).*

where we neglect interactions in the Klein-Nishina regime, i.e. with photons above $\varepsilon'_T \approx m_e c^2/\gamma'$.

Because the optical to X–ray photon spectrum is flatter than ε^{-2} most of the inverse Compton energy flux will occur near $E_\gamma \approx D\gamma'^2\varepsilon'_T = D\gamma' m_e c^2$, and so we use $E_\gamma \approx (2\varepsilon D/\varepsilon_B)^{1/2} m_e c^2$ with $\varepsilon = 2$ keV to obtain the ratio

$$t'^{\rm ICS}_{\rm cool}(\gamma')/t'^{\rm syn}_{\rm cool}(\gamma') \approx F_E(\varepsilon)/F_E(E_\gamma)\exp[\tau_{\rm tot}(E_\gamma)] \equiv \rho(D, B, t_{\rm var}). \quad (3)$$

The total blob-frame cooling time scale of electrons by both processes must be less than the Doppler factor multiplied by the observed variability time and this gives

$$[1 + \rho(D, B, t_{\rm var})]Dt_{\rm var} > t'^{\rm ICS}_{\rm cool}, \quad [1 + \rho(D, B, t_{\rm var})^{-1}]Dt_{\rm var} > t'^{\rm syn}_{\rm cool}. \quad (4)$$

These two equations give two constraints which have been added to Fig. 2(a). Separate curve are plotted corresponding to variability simultaneous with the TeV γ-rays occurring at 2 keV and 0.2 keV. The parameter space allowed by the variability time scale condition lies above the dot-dashed curves to the left of the dotted curves.

One further constraint arises from the condition that the maximum energy of electrons (determined by the maximum energy of synchrotron photons) must be higher than the maximum energy of γ-ray photons in the blob frame, i.e. $\gamma'_{\rm max} m_e c^2 > E_{\gamma,\rm max} D^{-1}$, with $\gamma'_{\rm max} = (2\varepsilon_{\rm s,max}/\varepsilon_B D)^{1/2}$, $\varepsilon_{\rm s,max}$ being the maximum energy of synchrotron photons. This condition requires B to be below the thick dashed line in Fig. 2(a).

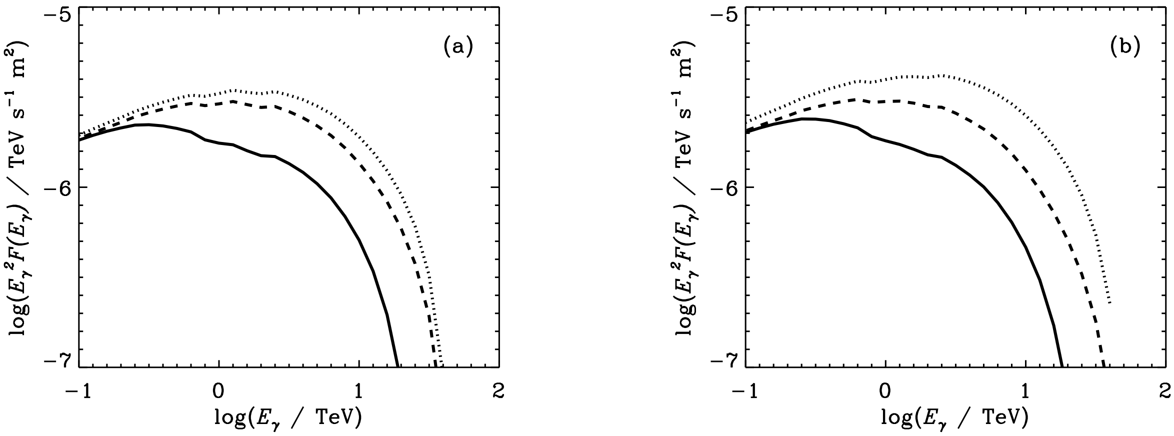

Figure 3: *(a) Best-fitting model with* $t_{\rm var} = 20$ *min for which* $B = 0.2$ *G and* $D = 20.4$*. Dotted curve shows the* γ*-ray spectrum produced in the blob by relativistic electrons. Dashed curve shows the* γ*-ray spectrum modified by absorption in the blob synchrotron radiation, i.e. the spectrum emerging from the blob. Full curve shows the* γ*-ray spectrum after propagation through the IRB using the lower IRB model. (b) Similar results for the best-fitting model with* $t_{\rm var} = 2.5$ *hr (*$B = 0.1$ *G and* $D = 11.5$*).*

5 Discussion and Conclusion

Not all of the parts of the thick solid curves within the "allowed" parameter space will actually give a viable SSC model as they may predict a high energy SED which may have a very different shape from that observed. Predicted spectra for each of the points labelled A, B, C, in Fig. 2(a) and normalized these to the observed flux at 1 TeV for the lower IRB model are shown in Fig. 2(b). Only point A is ruled out by the data, point B (for $B = 0.2$ G and $D = 20.4$) giving the best fit.

We emphasize the importance of including photon-photon absorption when determining the allowed parameters of the SSC model — e.g., in previous papers the energy at which the emitted energy flux per log energy interval maximizes in the γ-ray region is used when constructing constraints, as is the ratio of the peak luminosities. Neglecting absorption can lead to an incorrect determination of the allowed parameters. For example, we show in Fig. 3 that the maximum shifts to lower energies by about an order of magnitude when photon-photon absorption is included.

Our research is supported by the ARC and by Polish Komitet Badań Naukowych grant 2P03D 001 14.

References

Aharonian F. et al., 1998, A&A, 342, 69
Bednarek W., Protheroe R.J., 1997, MNRAS, 292, 646; 1999, MNRAS, in press, astro-ph/9902050
Catanese M. et al., 1997, ApJ, 487, L143; 1998, ApJ, 501, 616
Djannati-Atai A. et al., 1998, Abstracts of 19th Texas Symposium, Eds.: J. Paul et al. (CEA Saclay).
Dondi, L., Ghisellini, G., 1995, MNRAS, 273, 583
Kataoka J. et al., 1999, ApJ, 514, 138
Konopelko A. et al., 1999, Astropart.Phys. submitted, astro-ph/990193
Krawczynski H. et al., 1999, in Proc BL Lac Phenomenon, Turku, ed. L. Takalo, ASP Conf. Series
Krennrich F. et al., 1999, 511, 149
Malkan M.A., Stecker F.W., 1998, ApJ, 496, 13
Mattox, J. R. et al., 1993, ApJ, 410, 609
Pian E. et al., 1998, ApJ, 492, L17
Tavecchio F., Maraschi L., Ghisellini G., 1998, ApJ, 509, 608